Ising-like spin-$\frac{1}{2}$ quasi-one-dimensional antiferromagnets: Spin-wave response in $CsCoX_3$ salts

S. E. Nagler
Atomic Energy of Canada Ltd., Chalk River, Ontario K0J 1J0, Canada and University of Toronto, Toronto, Ontario N5S 1A7, Canada

W. J. L. Buyers
Atomic Energy of Canada Ltd., Chalk River, Ontario K0J 1J0, Canada

R. L. Armstrong
Atomic Energy of Canada Ltd., Chalk River, Ontario K0J 1J0, Canada and University of Toronto, Toronto, Ontario N5S 1A7, Canada

B. Briat
École Supérieure de Physique et Chimie Industrielles, 10 Rue Vauquelin, Paris, France
(Received 15 September 1982)

The spin-wave response of the $S=\frac{1}{2}$ Ising-like antiferromagnetic chain compounds $CsCoBr_3$ and $CsCoCl_3$ has been studied by inelastic neutron scattering. The asymmetry at low temperatures of the line shape of the spin-wave continuum is not correctly predicted by the existing theory of isolated chains to first order in the transverse exchange interaction. The effective spin Hamiltonian for a chain has been rederived and shown to include a slow internal staggered field from exchange mixing that influences the rapid spin fluctuations. Three-dimensional correlations are shown to be important above but close to Néel temperature. The first-order calculation of Ishimura and Shiba has been extended to include these effects and numerical calculations made for $0<T<J/k_B$. A good account is obtained of the spin-wave continuum and its temperature dependence. The results show that the highly asymmetric line shape arises from local staggered fields which vary on a much slower time scale than the transverse spin motion, and whose effect decreases with increasing temperature in the manner expected for the decay of the intrachain and interchain correlations. An improved and simplified account of the Zeeman ladder as seen in the Raman scattering at low temperatures has also been obtained.

I. INTRODUCTION

Recently there has been much interest in the dynamics of one-dimensional (1D) $S=\frac{1}{2}$ spin systems.[1-3] Their many unusual features include quantum effects, such as the spin-wave double continuum in the Heisenberg antiferromagnet, and the possibility of observing nonlinear excitations or "solitons." One of the most interesting systems is the Ising-like antiferromagnet, which has an exchange Hamiltonian

$$\hat{H}_{\rm ex}=2J\sum_i [S_i^z S_{i+1}^z+\epsilon(S_i^x S_{i+1}^x+S_i^y S_{i+1}^y)] ,$$
$$0<\epsilon<1 . \quad (1)$$

$CsCoBr_3$ and $CsCoCl_3$ are examples of quasi-1D Ising-like antiferromagnets with $\epsilon\sim 0.1$. The magnetic structure of both compounds has been determined by elastic neutron scattering,[4-6] and their magnetic susceptibility[6,7] has been measured as well as the specific heat of $CsCoBr_3$.[6] Spectroscopic studies on $CsCoCl_3$ have been carried out by neutron scattering,[8-13] infrared absorption,[14] and Raman scattering[15,16]; for $CsCoBr_3$ only the Raman spectrum[15,16] has been measured.

The spin dynamics of the Ising-like chain are dominated by the motion of domain walls.[17,18] For very small ϵ, the lowest-order ground state of the chain is the Néel state, with a total z component of spin $S_T^z=0$. Flipping ν adjacent spins of a Néel state creates a domain-wall–pair state. The first excited states of the system with energy $O(2J)$ above the Néel state and $S_T^z=0,\pm 1$, consist of superposi-

tions of the domain-wall—pair states.

At low temperatures the response measured in a neutron scattering experiment near $\omega \sim 2J$ arises from transitions from the ground state to the first excited states. The response is dominated by the transverse correlation function $S^{xx}(Q,\omega)$ and is therefore referred to as the spin-wave response. Also there are weak longitudinal fluctuations in this spectral range as shown by Fowler,[19] in contrast to the earlier results of des Cloizeaux and Gaudin.[20]

At temperatures where the excited states are thermally populated, one can observe additional low-frequency scattering from transitions within the band of excited states. Its spectrum is determined by the dynamics of propagating domain walls (solitons). The low-frequency response contains both longitudinal and transverse fluctuations analogous to critical scattering. The soliton response was observed in $CsCoCl_3$ (Ref. 13); in $CsCoBr_3$ it was recently found[21] to give rise to a well-defined peak as first predicted by Villain.[17] In this paper we consider only the spin-wave response.

Following some earlier work[8,9] the first high-resolution inelastic neutron scattering experiments on $CsCoCl_3$ revealed that the zone-center spin-wave response consisted of a continuum with a strong peak at its low-frequency end and a tail to higher frequencies.[10–13] The width of the continuum diminishes with wave-vector Q and a narrow peak is observed at the zone boundary. The behavior is an example of a quantum effect and is very different from the usual linear spin-wave response which consists of a sharp peak at all values of Q. The extent of the continuum was calculated exactly by Johnson *et al.*[22] The first theoretical prediction for the line shape of the spin-wave scattering arising from the continuum was the perturbation calculation of Ishimura and Shiba[18] (IS). Starting from the Ising limit, IS showed that to first order in ϵ the spin-wave spectrum of the Ising-like antiferromagnet at $T=0$ consists of a spin-wave continuum with maximum breadth at the zone center and zero width at the zone boundary. It should be noted that the des Cloizeaux—Gaudin spectrum does not form a lower bound to the excitation continuum of the Ising-like chain,[18,22] although it does for the Heisenberg chain.

The IS theory, however, does not account for the observed transverse scattering[10,12] in $CsCoCl_3$ at 25 K. The experimental line shapes are much more asymmetric than those predicted by IS. Further, the theory cannot describe the observed dispersion and bandwidth consistently with a single value of the parameter ϵ.[11] There are also some experimental problems due to the presence of phonon scattering in $CsCoCl_3$.

We report here results of an inelastic neutron scattering study of the spin-wave response in the isomorphous quasi-1D salt $CsCoBr_3$. The magnetic response in $CsCoBr_3$ is similar to that in $CsCoCl_3$, but the magnon response and phonon peaks are shifted relative to one another, enabling more definitive statements to be made regarding the discrepancy in the theoretical line shape. For the sake of completeness we present previously unpublished data on $CoCsCl_3$.

To improve upon the IS theory, the effective $S=\frac{1}{2}$ spin Hamiltonian for the Co^{2+} ion has been rederived taking account of the exchange mixing of higher levels within the ground doublet. In addition to the exchange interactions of Eq. (1), it is found that the Hamiltonian contains a staggered field whose effect on the spin-wave response depends on the local spin-spin correlations. It is further shown that interactions between the chains are important even above the three-dimensional (3D) Néel temperature, and must be included in a realistic calculation of the spin-wave response.

The improved theory is found to give a good account of the principal features of the spin-wave response of $CsCoBr_3$ and $CsCoCl_3$ up to temperatures $k_BT \sim J$. In addition, the results of Raman scattering experiments in $CsCoCl_3$ and $CsCoBr_3$ below the Néel temperature can be understood more fully and simply than before.

In Sec. II the experiments method and results are presented. In Sec. III the spin Hamiltonian is derived and $S^{xx}(Q,\omega)$ is calculated. The theoretical and experimental results are compared in Sec. IV.

II. MEASUREMENTS

The $CsCoCl_3$ crystal has been described earlier.[10] The single crystal of $CsCoBr_3$ was prepared from a stoichiometric amount of 48.6-g CsBr (Merck) and 50.0-g anhydrous $CoBr_2$ (Ventron) which was thoroughly dried in a quartz tube under HBr at temperatures up to 400 °C. The tube was then sealed under vacuum and slowly (1 cm per 24 h) lowered in a Bridgman furnace. The crystal is almost cylindrical with a height of 40 mm and diameter of 17 mm. Both compounds have a hexagonal structure with space group D^4_{6h} and lattice constants as indicated in Table I. The cobalt ions lie along chains in the c direction (Fig. 1) with two Co^{2+} ions per unit cell. At the upper Néel temperature T_{N_1} the magnetic structure becomes partially ordered with $\frac{2}{3}$ of the spin chains aligned in an antiferromagnetic triangular array and the other $\frac{1}{3}$ disordered (Fig. 2). At the lower temperature T_{N_2} the remaining $\frac{1}{3}$ of the chains order resulting in a hexagonal ferrimagnetic structure in the ab plane.[5,6]

TABLE I. Lattice constants and Néel temperatures.

	c (Å)	a (Å)	T_{N_1} (K)	T_{N_2} (K)
$CsCoBr_3$	6.26 (35 K)	7.45 (35 K)	28.3[a]	~ 10[a]
$CsCoCl_3$	6.00 (25 K)	7.14 (25 K)	20.8[b]	~ 13.5[b]

[a]Reference 6.
[b]Reference 5.

Each crystal was mounted in a cryostat so that its $(h,0,l)$ plane lay in the scattering plane of a triple axis spectrometer at the NRU reactor, Chalk River. All measurements were made with constant momentum transfer $\vec{K}$ and fixed scattered neutron energy E_1. The resolution conditions are given in Table II.

The spin-wave excitations were observed at several temperatures above the upper Néel temperatures T_{N_1} (Table I). Their magnetic character was confirmed by observing the decrease in their intensity as the momentum transfer increased, according to the magnetic form factor.

The 1D nature of the spin-wave response in $CsCoBr_3$ is clearly demonstrated by the dispersion of the peak frequencies shown in Fig. 3. Along the c^* direction the dispersion is marked and symmetric about the antiferromagnetic zone-boundary point. The zone boundary studied was at wave-vector transfer $\vec{K}=(0,0,2.5)2\pi/c$, for which the interspin phase difference is $Q=\pi/2$. The zone-boundary frequency is 3.47 ± 0.06 THz. No change in frequency was observed as $\vec{K}$ was varied along the a^* direction.

Some typical high-resolution line-shape scans are given in Fig. 4 for $CsCoCl_3$ and Figs. 5–8 for $CsCoBr_3$. We note the following features common to both compounds.

At temperatures just above the 3D antiferromagnetic transition temperature, the response at the antiferromagnetic zone center consists of a broad continuum strongly peaked at low frequencies, with a high-frequency tail extending beyond the zone-boundary frequency. The continuum becomes narrower as the wave vector increases and becomes a resolution-limited peak at the zone boundary. As seen in Figs. 6 and 8, the shape of the response at the nuclear zone center in $CsCoBr_3$ is very similar to that at the antiferromagnetic zone center except for the overall intensity. The same result was found in $CsCoCl_3$.

As the temperature is increased, the low-frequency peak in the zone-center response shows a drastic reduction in intensity. The resulting line shape is much less asymmetric. The same behavior is observed for other wave vectors but to a lesser extent, as seen in Fig. 4 for $CsCoCl_3$. The integrated intensity under the zone-boundary peak also decreases markedly. At all wave vectors, however, the spin-wave scattering persists to high temperatures and is readily observed as a peak at 80 K ($T\sim J/k$).

As has been discussed previously, phonon scattering affects the observed line shape in $CsCoCl_3$. Referring to Fig. 9 we see that the (0,0,3) profile exhibits a second peak at a frequency of ~ 3.7 THz. The peak is due to phonon scattering as shown by its $\vec{K}$ dependence in Fig. 10. The phonon is also visible at the zone boundary with very little if any change in frequency. The Raman scattering results of Johnstone *et al.*[23] indicate that the zone-center E_{1g} phonon in $CsCoCl_3$ has a frequency of about 3.8 THz,

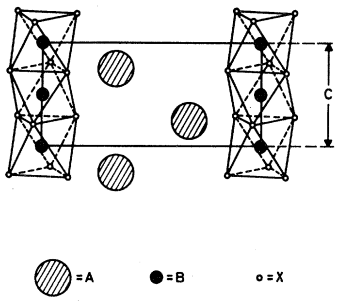

FIG. 1. Structure of $CsCoX_3$ salts. Here $A\equiv$Cs, $B\equiv$Co, and $X\equiv$Cl or Br.

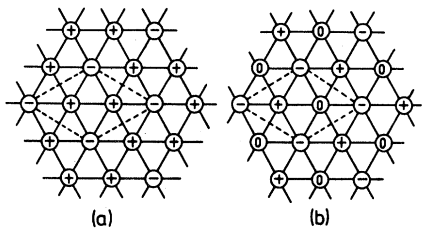

FIG. 2. Magnetic structure in ab plane below T_{N_1}. (a) Ferrimagnetic structure for $T<T_{N_2}$. (b) Structure for $T_{N_2}<T<T_{N_1}$. Chains marked ○ are disordered (after Ref. 5).

TABLE II. Spectrometer configurations.

Specimen	$CsCoCl_3$	$CsCoBr_3$
Spectrometer	$L3$	$N5$
Monochromator	Ge(113)	Si(111)
Analyzer	Graphite(002)	Si(111)
Collimation		
before specimen	0.6°	0.4°
after specimen	0.7°	0.7°
E_1	2.6 THz	3.0 THz
Full width at half maximum of spin-wave peak at zone boundary	0.25 THz	0.36 THz

in reasonable agreement with our data (Lehmann *et al.*[15] measure 3.54 Thz), and is very strongly coupled to the magnon scattering. The coupling may explain, through its effect on the temperature and wave-vector dependence, why it was unrecognized in the experiment of Satija *et al.*[12] Their experiment was, however, in a different scattering plane ($\xi\,\xi\,\eta$). The presence of the phonon makes it difficult to extract the true zone-center line shape for $CsCoCl_3$.

Figures 6–8 show that phonon peaks are also present within the spin-wave band of $CsCoBr_3$. The sharp peak at 4.37 THz in the (003) antiferromagnetic zone-center scan is clearly a phonon. However, it seems to be uncoupled from the magnetic scattering. The weak peak at 2.2 THz is very likely the E_{1g} phonon, which was observed at 2.17 THz in Raman scattering. The phonon is again strongly coupled to the magnetic scattering, as is evident from the temperature dependence (Fig. 6). As in $CsCoCl_3$, the phonon is clearly seen at the zone boundary (Fig. 7). Since the strongly coupled E_{1g} phonon lies essentially below the spin-wave band scattering in $CsCoBr_3$, it would seem that $CsCoBr_3$ is a better candidate for comparison of neutron scattering experiments with detailed theories of the magnetic response as pointed out by Lehmann *et al.*[15]

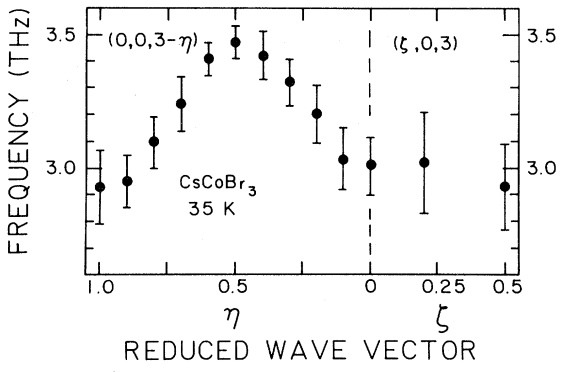

FIG. 3. Peak frequencies observed in the $CsCoBr_3$ spin-wave response at 35 K.

From Figs. 3–8, it is apparent that a proper theory of magnetic response in the paramagnetic region of the $CsCoX_3$ salts must explain the following results:

(1) The presence and dispersion of the strong peak at the low-frequency end of the spectrum at lower temperatures.

(2) The extent of the continuum scattering as a function of Q.

(3) The observation that although the spin-wave response at all wave vectors persists up to temperatures as great as J/k_B or larger, the line shape near the zone center become smoother and less asymmetric as the temperature is raised.

III. THEORY

The derivation of an effective spin Hamiltonian for the $CsCoX_3$ salts is complicated by the unquenched orbital angular momentum of the cobalt ion. The Co^{2+} ion is situated in an octahedron of X ions with a slight trigonal distortion (Fig. 1). The strong cubic crystal field causes the lowest lying ^4F configuration to break up into manifolds with the $^4T_1$ state lowest followed by states of $^4T_2$ and $^4A_2$ symmetry.[24] The higher-lying ^4P multiplet has $^4T_1$ symmetry, and therefore is mixed with the ground $^4T_1$ multiplet within which the orbital angular momentum is $\vec{L}=\alpha\vec{l}$ in terms of an effective $l=1$ with $\alpha=-1.428$.[25] Within the twelvefold-degenerate ground state the magnetic Hamiltonian is

$$\hat{H}'=\hat{H}_{\rm ion}+\hat{H}_{\rm ex}\ . \tag{2}$$

Here $\hat{H}_{\rm ion}$ is the single-ion Hamiltonian containing the spin-orbit interaction and trigonal distortion terms,

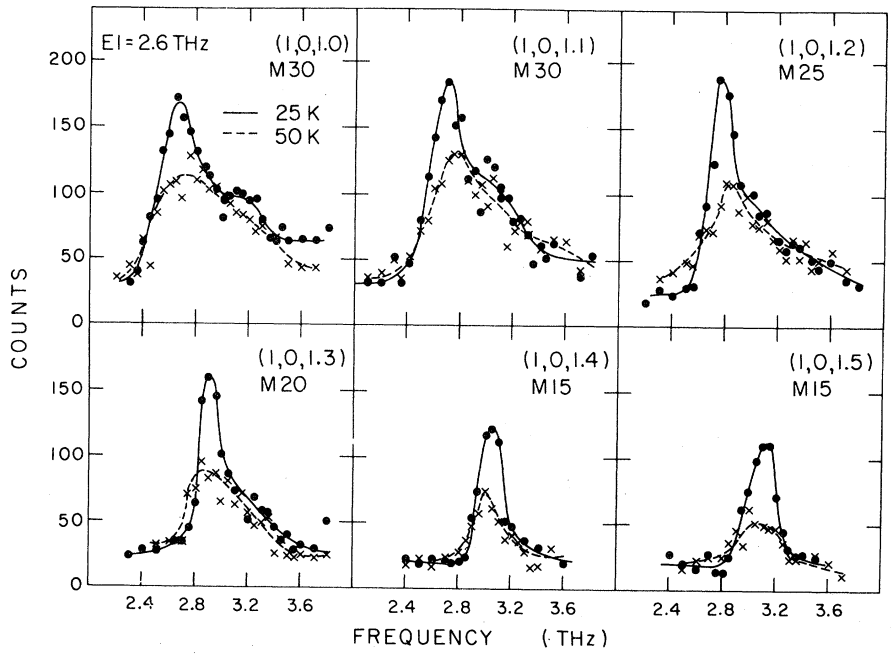

FIG. 4. $CsCoCl_3$ line-shape scans. Monitor M is a measure of the number of incident neutrons. Lines are guides to the eye.

$$\hat{H}_{\text{ion}} = \sum_i [\alpha k \lambda \vec{l}_i \cdot \vec{T}_i - \delta[l_i^{z^2} - \tfrac{2}{3}]]. \quad (3)$$

Here $\vec{T}_i$ is the $T = \frac{3}{2}$ true spin, λ the spin-orbit coupling constant, $k = 0.91$ is the orbital reduction factor,[26] and δ is the trigonal distortion parameter. $\hat{H}_{\text{ion}}$ breaks up the $^4T_1$ manifold into six Kramers doublets. The projection of the exchange Hamiltonian $\hat{H}_{\text{ex}}$ into the lowest-lying doublet leads to the effective $S = \frac{1}{2}$ Hamiltonian. The derivation of the effective Hamiltonian for $CsCoCl_3$ was discussed by Tellenbach,[8] but he ignored the effect of exchange mixing which, as is shown below, is important in the $CsCoX_3$ salts.

The exchange interaction between real spins has

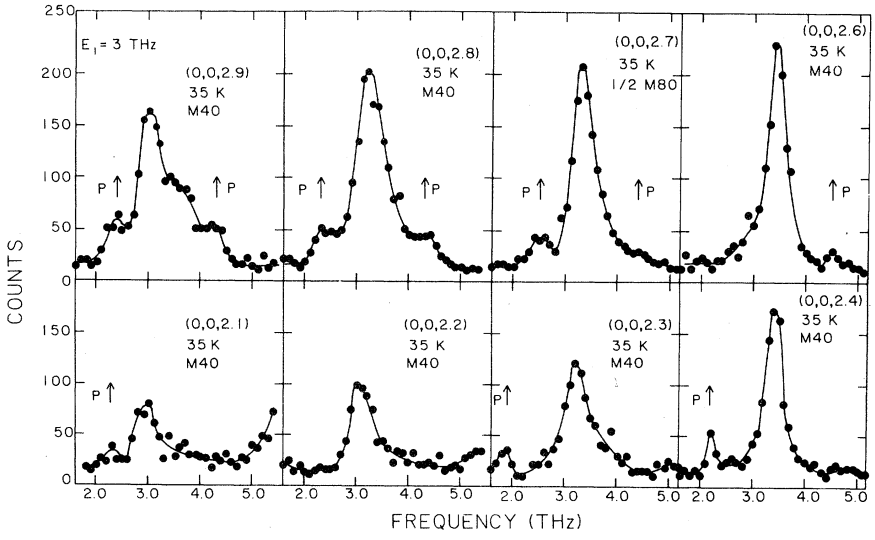

FIG. 5. $CsCoBr_3$ typical line-shape scans at 35 K. Known phonons are marked with P. Lines are guides to the eye. The notation $\frac{1}{2}M80$ denotes counts with the percentage accuracy of a monitor 80 counting time, divided by 2 for comparison with the other data.

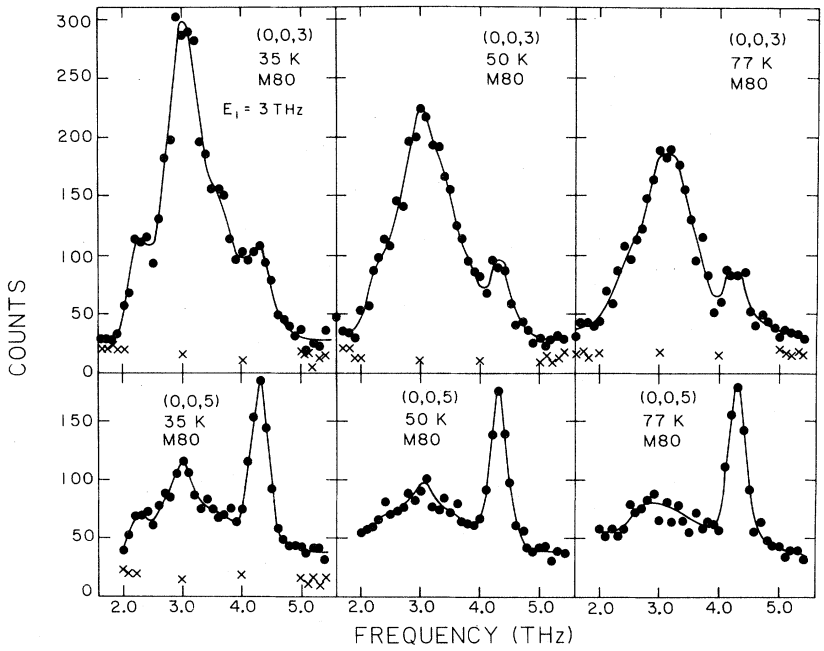

FIG. 6. $CsCoBr_3$ line-shape scans at the antiferromagnetic zone center. Crosses represent fast-neutron background measurements performed by inserting cadmium into the neutron beam. Lines are guides to the eye.

been found[26,27] to be largely of the isotropic form

$$\hat{H}_{\rm ex}=\sum_{i,j} I_{ij}\vec{\mathrm{T}}_i\cdot\vec{\mathrm{T}}_j \ . \tag{4}$$

The nearest-neighbor exchange constant within a chain, I, is much greater than that between chains, I' $[(I'/I)\sim 10^{-2}]$.[28,29] For a single chain we have

$$\hat{H}_{\rm ex}=2I\sum_i \vec{\mathrm{T}}_i\cdot\vec{\mathrm{T}}_{i+1} \ . \tag{5}$$

A. Field due to exchange mixing

At low temperatures where there is a 3D ordered spin structure the molecular field at each site causes

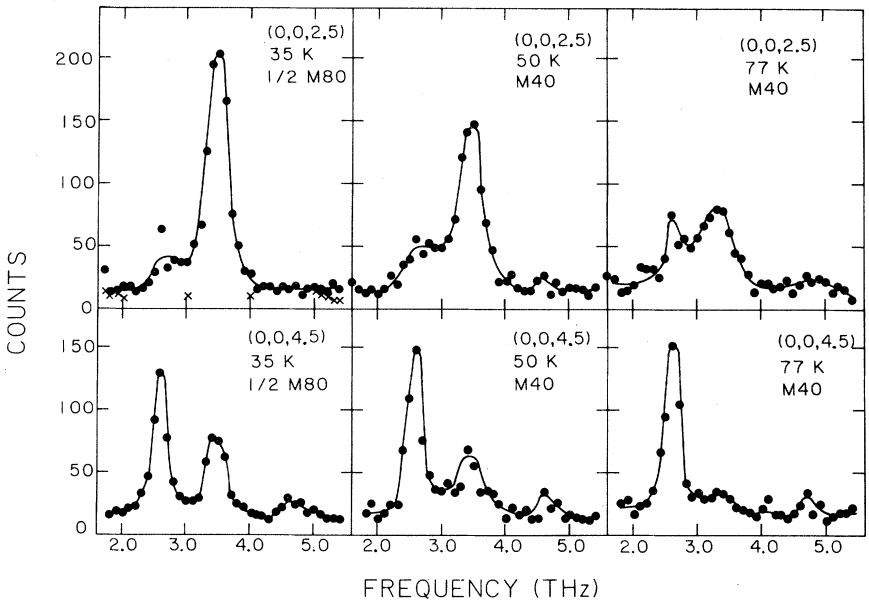

FIG. 7. $CsCoBr_3$ line-shape scans at the zone boundary. Lines are a guide to the eye.

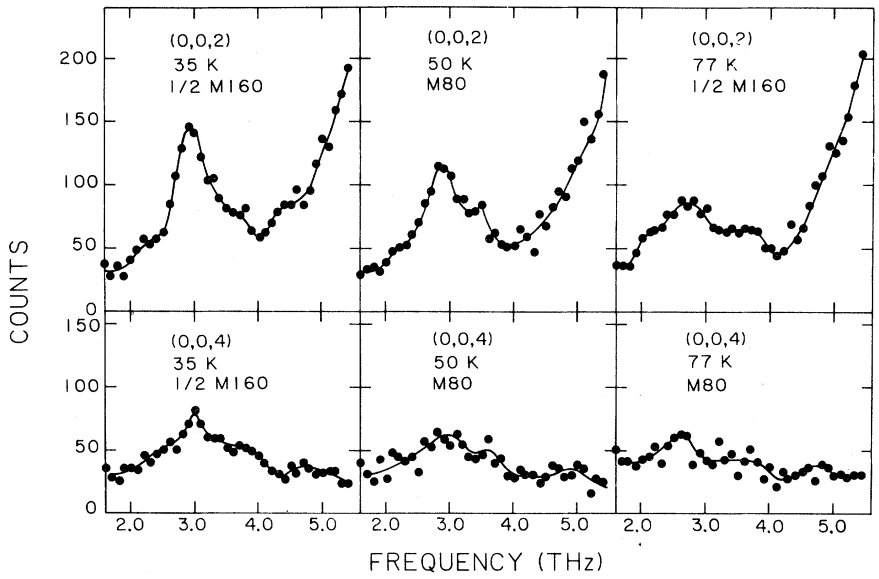

FIG. 8. $CsCoBr_3$ line-shape scans at the nuclear zone center. Sharp rise starting at 4.0 THz in the (0,0,2) scan is due to small angle scattering. Lines are guides to the eye.

exchange mixing of the single-ion levels. Since this is a local effect it is also present in the paramagnetic region as a slowly fluctuating field and is especially important in 1D systems because of their strong short-range order.

The exchange mixing results in an asymmetry between the true-spin matrix elements of the two lowest-lying levels. The mixing is accounted for in the transformation to effective spin $S=\frac{1}{2}$ variables by the relations

$$T^z=\Delta S^z+\Sigma\ ,$$
$$T^{\pm}=\gamma S^{\pm}\ , \tag{6}$$

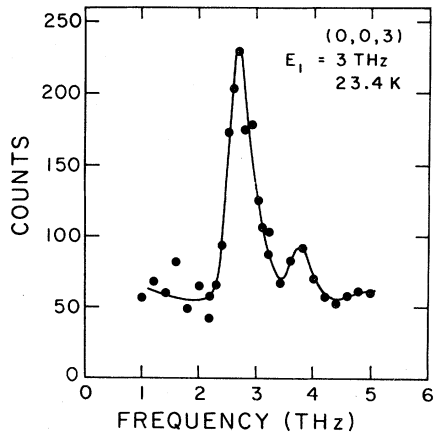

FIG. 9. $CsCoCl_3$ line shape at the antiferromagnetic zone center. Line is a guide to the eye.

for a spin-up site, where

$$\Delta=\langle 0\,|\,T^z\,|\,0\rangle-\langle 1\,|\,T^z\,|\,1\rangle\ ,$$
$$\Sigma=\tfrac{1}{2}(\langle 0\,|\,T^z\,|\,0\rangle+\langle 1\,|\,T^z\,|\,1\rangle)\ , \tag{7}$$
$$\gamma=\langle 1\,|\,T^-\,|\,0\rangle=\langle 0\,|\,T^+\,|\,1\rangle\ .$$

For a spin-down site we write

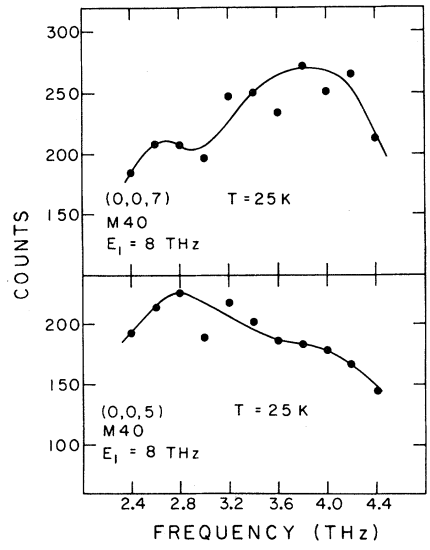

FIG. 10. $CsCoCl_3$ low-resolution scans at the antiferromagnetic zone center. Note the growth in intensity of the upper peak at (0,0,7) as opposed to (0,0,5), showing the phonon nature of the scattering. Lines are guides to the eye. See Ref. 11 for the comparison of (0,0,3) and (0,0,5).

$$T^z=\Delta S^z-\Sigma\ ,$$
$$T^{\pm}=\gamma S^{\pm}\ . \tag{8}$$

In the expressions above $|0\rangle$ and $|1\rangle$ are the single-ion ground and excited states at the up site.

The real spins in Eq. (5) are replaced by the effective $S=\frac{1}{2}$ spins to give an exchange Hamiltonian

$$\hat{H}_{\rm eff}=2J\sum_i[S_i^zS_{i+1}^z+\epsilon(S_1^xS_{i+1}^x+S_1^yS_{i+1}^y)]$$
$$+h_0\sum_i S_i^z(-1)^i+C_0\ , \tag{9}$$

where

$$2J=2I\Delta^2\ ,$$
$$\epsilon=(\gamma/\Delta)^2\ ,$$
$$h_0=4I\Delta\Sigma\ , \tag{10}$$
$$C_0=2NI\Sigma^2\ .$$

Exchange mixing thus leads to a uniform staggered-field term in the effective $S=\frac{1}{2}$ Hamiltonian. The field h_0 is a single-ion effect and is not due to interactions between different chains of spins. The importance of this term for the transverse-spin dynamics depends crucially on the time scale for the decay of the excited state. If the time required for a readjustment of the single-ion levels of the excited ion is much larger than the period of the excitation, $\tau\simeq 1/2J$, the term must be included. The readjustment of the single-ion levels is governed by the time τ_s necessary for the local spin correlations to change. Empirically, this can be estimated from the width $\Delta\omega$ in frequency of the quasielastic scattering at the ordering wave vector $Q=\pi$. If $1/\tau_s\sim\Delta\omega\ll 2J$ (the excitation energy) the uniform-field term should be included. In terms of the effective $S=\frac{1}{2}$ model, we have $\Delta\omega\sim\kappa\epsilon J$ where $2\pi\kappa^{-1}$ is the correlation length in units of the interspin distance.[17] The condition becomes $\kappa\epsilon J\ll 2J$. This condition is easily satisfied in the $CsCoX_3$ salts.

A reasonable upper limit for the effect of exchange mixing is given by the molecular-field approximation solution for the single-ion levels. The true-spin Hamiltonian

$$\hat{H}^i_{\rm mf}=\hat{H}^i_{\rm ion}+4I\langle T_n^z\rangle T_i^z\ , \tag{11}$$

where n represents a neighbor of atom i, is diagonalized in an iterative manner, since $\langle T_n^z\rangle$ depends on the eigenstates.[26] The choice of parameters in Eq. (3), was as follows. The free-ion value of λ (-5.34 THz) (Ref. 30) was assumed, with k of Ref. 26, α of Ref. 25, and δ was chosen to give the value of ϵ that best describes the 80-K data (see Sec. IV).

The dependence of the parameters of the effective Hamiltonian on the molecular-field-induced exchange mixing is clearly indicated in Fig. 11. The staggered field h_0 increases monotonically with $H_m=4I\langle T^z\rangle$ and has a nearly linear dependence on the molecular field. The field h_0 is therefore expected to decrease as the temperature increases; as a rough guide we may expect $h_0\sim\langle S_0^zS_1^z\rangle\sim e^{-\kappa}$.

The anisotropy parameter ϵ is also an increasing function of molecular field. Therefore, the effective value of ϵ for the $CsCoX_3$ salts will decrease as the temperature is raised.

B. Coupling between chains

Until now, we have ignored the effect of interchain exchange interactions. As will be discussed in the next section, the interchain coupling is important for the understanding of spin dynamics in the $CsCoX_3$ salts. In terms of the effective $S=\frac{1}{2}$ model the nearest-neighbor part of the interchain exchange coupling leads to a term in the Hamiltonian of one chain,

$$\hat{H}^{\rm ic}_{\rm ex}=2J'\sum_i\sum_\delta S_i^zS_{i+\delta}^z\ , \tag{12}$$

where δ is a nearest neighbor in the same ab plane as atom i. The transverse coupling is neglected as it is smaller by a factor $\sim\epsilon$. It is reasonable to treat the interchain interactions in the molecular-field ap-

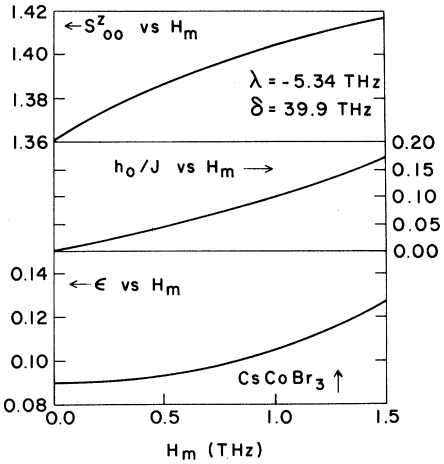

FIG. 11. Exchange-mixing effects in the molecular-field approximation. The spin-orbit coupling parameter is $\lambda=-5.39$ THz. The trigonal distortion parameter is $\delta=39.9$ THz. Arrow indicates the value of molecular field (H_m) which reproduces the observed zone-boundary spin-wave energy for $CsCoBr_3$. Note $S^z_{00}\equiv\langle 0\,|\,T^z\,|\,0\rangle$.

proximation.[31] The effect is to add to the effective spin Hamiltonian a term

$$\hat{H}^{\rm ic}=h_{\rm ic}\sum_i S_i^z(-1)^i\ , \tag{13}$$

where

$$h_{\rm ic}=2J'\sum_\delta \langle S^z_{i+\delta}\rangle\ .$$

At temperatures well above T_{N_1} this term drops rapidly to zero, but at temperatures just above T_{N_1} the interchain field is expected to have the form

$$h_{\rm ic}\simeq h_{\rm ic}(T=0)e^{-\kappa_\perp}\ , \tag{14}$$

where $2\pi\kappa_\perp^{-1}$ is the in-plane spin-correlation length. With the inclusion of exchange mixing and interchain interactions in the molecular-field approximation, the effective $S=\frac{1}{2}$ spin Hamiltonian for isolated chains of cobalt ions in $CsCoX_3$ salts is

$$\hat{H}_{\rm eff}=2J\sum_i[S_i^zS_{i+1}^z+\epsilon(S_i^xS_{i+1}^x+S_1^yS_{i+1}^y)]+h\sum_i(-1)^iS_i^z\ , \tag{15}$$

where $h=h_0+h_{\rm ic}$.

C. Neutron scattering and spin dynamics

For a spin chain along the $\hat{z}$ direction, the magnetic neutron inelastic scattering cross section can be written

$$\frac{d^2\sigma}{d\Omega\,d\omega}\propto|f(\vec{\rm K})|^2\sum_{\alpha\beta}(\delta_{\alpha\beta}-\hat{K}_\alpha\hat{K}_\beta)S^{\alpha\beta}(Q,\omega)\ , \tag{16}$$

where $\vec{\rm K}$ is the momentum transfer, $Q=(\vec{\rm K}-\vec{\tau})\cdot\hat{z}c/2$ is the reduced 1D wave vector measured from a nuclear reciprocal-lattice vector $\vec{\tau}$, $f(\vec{\rm K})$ the magnetic form factor, and

$$S^{\alpha\beta}(Q,\omega)=\frac{1}{2\pi}\int\sum_j e^{i\omega t}e^{iQj}\langle S_0^\alpha(0)S_j^\beta(t)\rangle dt$$

is the dynamic spin–spin-correlation function. The spins along the chains are labeled by j, and Q is the interspin phase difference. The dynamic response $S^{xx}(Q,\omega)$ can be calculated based on the Hamiltonian of Eq. (15). If the ground state $|G\rangle$ and excited states $|E\rangle$ at an energy E above the ground state are known, then at $T=0$,

$$S^{\alpha\alpha}(Q,\omega)=\sum_E|\langle E|S_Q^\alpha|G\rangle|^2\delta(\omega-E)\ , \tag{17}$$

where

$$S_Q^\alpha=\frac{1}{\sqrt{N}}\sum_j e^{iQj}S_j^\alpha\ .$$

Following IS, perturbation theory is developed from the Ising limit by writing

$$\hat{H}_{\rm eff}=\hat{H}_0+\hat{H}_1\ ,$$
$$\hat{H}_0=2J\sum_i S_i^zS_{i+1}^z+h\sum_i(-1)^iS_i^z\ , \tag{18}$$
$$\hat{H}_1=2\epsilon J\sum_i(S_i^xS_{i+1}^x+S_i^yS_{i+1}^y)\ .$$

The ground state of $\hat{H}_0$ is a Néel state $|N\rangle$, with the z component of total spin $S_T^z=0$. The first excited states with $S_T^z=0,\pm1$ are the domain-wall–pair states discussed by IS. Consider the states with $S_T^z=+1$. These are labeled $|\nu,Q\rangle$ where $\nu=1,3,5,\ldots,N-1$ is the length of the domain within which the spins are flipped with respect to the Néel state and Q is the wave vector characterizing the state. In first order the perturbed ground state is

$$|G\rangle\simeq|N\rangle+\frac{1}{E_N-\hat{H}_0}\hat{H}_1|N\rangle\ . \tag{19}$$

The first excited states are found by diagonalizing the matrix defined by

$$\langle\nu',Q'|\hat{H}_{\rm eff}|\nu,Q\rangle=\delta_{Q',Q}[(2J+h\nu)\delta_{\nu',\nu}+\epsilon J(1+e^{-2iQ})\delta_{\nu',\nu-2}+\epsilon J(1+e^{2iQ})\delta_{\nu',\nu+2}]\ . \tag{20}$$

In Eq. (20) the state $\nu=1$ is coupled only to the state $\nu=3$ and not to the state $\nu=N-1$.

Unlike other authors[15–17] we have not included the second-order matrix elements occurring within the manifold of first excited states. The reason is that in second order, the states of energy $O(4J)$ will be coupled to the domain-wall–pair states of energy $O(2J)$. For a chain of N spins there are $O(N^2)$ states at $2J$, but $O(N^4)$ states at $4J$. For large N the coupling to these higher-energy states will likely be more important than the second-order coupling within the domain-wall–pair states. It is therefore more consistent to use only first-order perturbation theory when the basis is restricted to the domain-wall–pair states. Using Eqs. (17) and (18) we can write

$$S^{xx}(Q,\omega)=\tfrac{1}{4}\sum_E\left[\left[1-\frac{\epsilon J\cos Q}{J+h}\right]^2|\langle E|1Q\rangle|^2+\left[\frac{\epsilon J\cos Q}{J+h}\right]^2|\langle E|3Q\rangle|^2 -2\left[1-\frac{\epsilon J\cos Q}{J+h}\right]\left[\frac{\epsilon J\cos Q}{J+h}\right]{\rm Re}(\langle E|3Q\rangle\langle 1Q|E\rangle e^{iQ})\right]\delta(\omega-E)\ . \tag{21}$$

The expression is obtained by retaining terms of order ϵ in the eigenstates and energies. In the limit where $h \to 0$, IS have calculated $S^{xx}(Q,\omega)$ analytically. The response at constant Q is a broad slightly asymmetric frequency distribution whose width tends to zero at the zone boundary. With $h \neq 0$, the continuum breaks up into sharp modes corresponding to the "Zeeman ladder" discussed by Shiba.[28] The expression in Eq. (21), although for $T=0$, should be a good approximation to the observed transverse-spin-wave response in the $CsCoX_3$ salts for $T \ll 2J/k_B$. Proper account must be taken, however, of the changes in the effective spin Hamiltonian caused by the temperature dependence of the exchange mixing as well as the influence of 3D correlations. We now turn to a discussion of the calculated results for $S^{xx}(Q,\omega)$ over the temperature range $0 < T \lesssim J/k_B$ and a comparison of the theory with inelastic neutron scattering and Raman scattering experiments.

IV. DISCUSSION

To show that for the region $T \lesssim J/k_B$ the $T=0$ expression for the spin-wave-like scattering, Eq. (20), is a reasonable approximation, a simple estimate of the depopulation of the ground state is given by considering only the single-ion levels. For low temperatures the fraction of Co^{2+} ions in the ground state is

$$f \approx (1+e^{-2J/k_B T})^{-1} .$$

When $T \sim J/k_B$, $f \simeq 0.9$, so that at temperatures up to 80 K for $CsCoBr_3$ and $CsCoCl_3$ we expect that the spin-wave response is dominated by transitions from the ground state. The above may somewhat underestimate f because of the high degeneracy of the excited states in the interacting system, but is expected to give a rough guide to the behavior.

We recall that at temperatures just above the Néel temperature, the zone-center response of the $CsCoX_3$ salts consists of a sharp peak with a high-frequency tail. As the temperature is raised to $T \sim 2T_{N_1}$ the intensity of the sharp peak decreases much more rapidly than that of the tail.

Given that the response of the pure 1D chain should not change drastically over this temperature range, it is likely that the sharp peak arises from strong 3D correlations which persist even above T_{N_1} as shown below.

Since the parameters of the effective spin Hamiltonian depend crucially on the extent of exchange mixing and the presence of 3D correlations, the calculation of the spin-wave response is considered in three different regimes:

(1) The high-temperature limit $T \gtrsim 2T_{N_1}$.

(2) The ordered phase $T < T_{N_1}$.

(3) The intermediate regime $2T_{N_1} > T \gtrsim T_{N_1}$.

In the high-temperature regime it may be safely assumed that 3D correlations are absent, so that $h_{ic}=0$. There may still be some exchange mixing, but it will be very small and for simplicity we assume that $h_0=0$. There is now no uniform staggered field, and the analytic theory of IS for $S^{xx}(Q,\omega)$ may be applied

The first excited states form a continuum with upper and lower bounds given to first order in ϵ by

$$\omega_{\pm} = 2J(1 \pm 2\epsilon \cos Q) , \tag{22}$$

as shown in Fig. 12. Figures 13 and 14 show the results of fits of the IS theory to our results at high temperature, for $CsCoBr_3$ at 77 K, and for $CsCoCl_3$ at 50 K. The wave vector is that of the antiferromagnetic zone center, $Q=\pi$. The solid line is the IS theory convoluted with a Gaussian to account for the spectrometer resolution (Table II). A flat fast-neutron background has been subtracted from the data. The theory fits remarkably well, in contrast to the situation at 25 K for $CsCoCl_3$ to which this theory has previously been applied.[11,12,13] The fitted parameters are, for $CsCoBr_3$,

$$J = 1.621 \pm 0.007, \quad \epsilon = 0.098 \pm 0.003$$

and for $CsCoCl_3$,

$$J = 1.495 \pm 0.010, \quad \epsilon = 0.088 \pm 0.004$$

with J in units of THz. From these values of ϵ and the free-ion value of $\lambda = -5.34$ THz it follows[24] for zero molecular field that δ is 39.9 THz for $CsCoBr_3$ and 42.2 THz for $CsCoCl_3$. The trigonal distortion parameters should be independent of temperature, as are the exchange constants J, but the anisotropy ϵ should increase at lower temperatures because of exchange mixing.

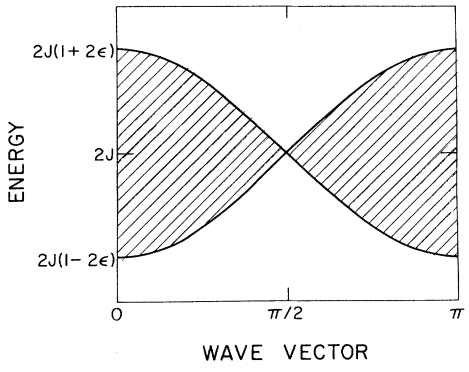

FIG. 12. Continuum of first excited states as described in the text.

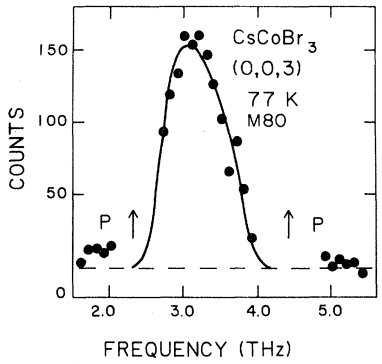

FIG. 13. Fit of IS theory to $CsCoBr_3$ antiferromagnetic zone-center scattering in the high-temperature regime. Arrows mark positions of phonon scattering not included in the fit. Theoretical line is described in the text. Dashed line is the background level.

Now consider the low-temperature, magnetically ordered region. Exchange mixing is appreciable and the uniform field term h_0 will be present. In addition, the interchain field h_{ic} is nonzero but differs for each chain according to the local environment. In the presence of the staggered field the excitation continuum breaks up into a set of discrete energy levels, the Zeeman ladder described by Shiba.[28] The resulting $S^{xx}(Q,\omega)$ is given by a superposition of a set of sharp modes. Evidence for such structure was indeed seen in the spin-wave response of $CsCoCl_3$ at 4.2 K.[10] The actual energies of the Zeeman ladder at $Q=0$, however, can be measured much more accurately by Raman scattering.

Raman scattering experiments have been performed by Lehmann *et al.*[15] and Johnstone *et al.*[16] on both $CsCoBr_3$ and $CsCoCl_3$ in the temperature regions $T<T_{N_2}$ and $T_{N_2}<T<T_{N_1}$. The results were interpreted in terms of the Zeeman ladder, but the effect of exchange mixing was neglected.

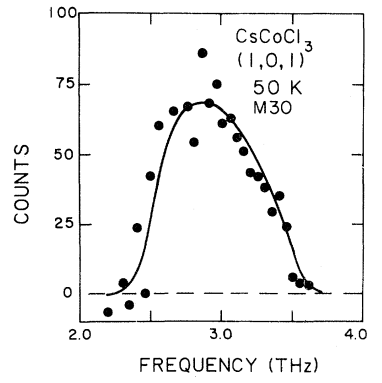

FIG. 14. Fit of IS theory to $CsCoCl_3$ antiferromagnetic zone-center scattering in the high-temperature regime.

Consider the postulated magnetic structure of the $CsCoX_3$ salts for $T<T_{N_2}$.[5,6] In the ferrimagnetic structure $\frac{2}{3}$ of the chains will have a staggered field $h_{ic}=0$ and the remaining $\frac{1}{3}$ will have $h_{ic}=6J'$. In the region $T_{N_2}<T<T_{N_1}$ $\frac{1}{3}$ of the chains will be disordered. In this temperature region, however, the characteristic time of flipping of the spins ($\tau_s^{-1}\sim\kappa\epsilon J$) will be slow, and the correlation length along the chain will be large. If the condition $J'e^{-\kappa_\perp}>\tau_s^{-1}$ is satisfied, the molecular field due to the disordered chains can be viewed as quasistatic.[28] Using the Ising-model result for κ this condition becomes, for low T and $\kappa_\perp=0$,

$$T<J/[k_B\ln(2\epsilon J/J')] .$$

This condition holds for $CsCoCl_3$ and $CsCoBr_3$ below T_{N_1} using the parameters of Table III. Under this condition it can be assumed that a spin in the disordered chain is either up or down with probability $\frac{1}{2}$. There are now four possible values of the field h_{ic} with probabilities as indicated in Table IV, giving rise to four distinct sets of lines. One expects that the series of lines A ($h=h_0+6J'$) and C ($h=h_0$) will decrease in intensity when T goes from $T<T_{N_2}$ (I) to $T_{N_2}<T<T_{N_1}$ (II), while the series B_1 ($h=h_0+4J'$) and B_2 ($h=h_0+2J'$) will gain in intensity.

Previous authors[15,16,28] have ignored exchange mixing, and used $h_0=0$, for which one expects only the A and B lines plus a continuum. However, the C lines have in fact been observed. Lehmann *et al.*[15] have noted that in both $CsCoBr_3$ and $CsCoCl_3$, the onset of the expected continuum was not smooth but rather occurs as a sharp shoulder which decreases in intensity on warming from (I) to (II). We claim that this feature is in fact the lowest-lying C line. Johnstone *et al.*[16] also observed the C line in $CsCoBr_3$, and attempted to explain it as an effect of fluctuations. The present explanation is simpler and leads to a more consistent interpretation of the spectra as discussed below.

Both Lehmann *et al.*[15] and Johnstone *et al.*[16] had difficulty fitting the observed spectra well with a unique choice of ϵ and J'. Lehmann *et al.* fixed J and J', and varied ϵ for each of the series of lines. On the other hand, Johnstone *et al.* fixed J, ϵ, and effectively varied J' for each series. Neither procedure is physically reasonable. With the spin Hamiltonian as described earlier, including the internal field through the parameter h_0, we find that the lines of all series can be described very well with a single choice of J, ϵ, J', and h_0. Table V shows the results of a fit to the lines observed by Lehmann *et al.* (LBW). As mentioned earlier, J was fixed by

TABLE III. Parameters of the spin Hamiltonian.

	$CsCoBr_3$			$CsCoCl_3$		
	$T \lesssim T_{N_2}$	35 K	77 K	$T \lesssim T_{N_2}$	25 K	50 K
J	1.62	1.62	1.621±0.007[a]	1.495	1.495	1.495±0.01[a]
ϵ	0.137±0.005	0.137	0.098±0.003[a]	0.120±0.003[a]	0.120	0.088±0.004[a]
$\frac{h_0}{J}$	0.020±0.003[a]	0.016	0.0	0.013±0.001[a]	0.012	0.0
$\frac{J'_{\text{eff}}}{J}$	0.059±0.002[a]	0.027[a]	0.0	0.020±0.001[a]	0.012[a]	0.0

[a]Indicates a fitted parameter. Errors are purely statistical.

the high-temperature neutron results, while h_0, ϵ, and J' were allowed to vary to yield the best fit values of Table III. The fit of LBW using different values of ϵ is also shown for comparison. The value of ϵ needed by LBW varies from 0.096 in no field to 0.144 with $h = h_0 + 6J'$ for $CsCoCl_3$, and from 0.160 to 0.235 for $CsCoBr_3$. The variation in ϵ is far too large to be explained by a difference in the exchange mixing for each type of chain.

Our fitted values of ϵ of 0.137 for $CsCoBr_3$ and 0.120 for $CsCoCl_3$ are greater than the high-temperature values as expected. When the single-ion–field term h_0 is included, three parameters need to be varied to explain 11 lines observed in $CsCoBr_3$ and 14 in $CsCoCl_3$. In addition, the previously unexplained C feature is easily accounted for. We conclude that the model provides a satisfactory description of the Raman scattering experiments in the ordered phase. The agreement confirms our hypothesis that the internal fields from exchange mixing as well as from interchain coupling should be included in the spin Hamiltonian for $CsCoX_3$ compounds.

Consider now the spin-wave response in the intermediate-temperature region $T \gtrsim T_{N_1}$. For an array of weakly interacting spin chains, two-dimensional correlations in the plane perpendicular to the chains will become important when $\xi_\perp > d_\perp$, the nearest-neighbor spin distance in the plane. According to the Ginzburg criterion applied to this system[31] this will be true in the temperature region

$$|T - T_{N_1}| / T_{N_1} \lesssim k_B T_{N_1} / J \ .$$

Applied to $CsCoBr_3$, this implies that interchain correlations should be important for $T \lesssim 38$ K, and for $CsCoCl_3$ for $T \lesssim 28$ K. The effect of interchain interactions must therefore be considered when we calculate the spin-wave response of $CsCoCl_3$ at 25 K and $CsCoBr_3$ at 35 K.

At temperatures just above T_{N_1}, the magnetic correlations will predominantly have the pattern of the spin structure in Fig. 2(b), with $\frac{1}{3}$ of the chains disordered and the other $\frac{2}{3}$ antiferromagnetically aligned. However, it is unlikely that the quasistatic approximation will be valid for the disordered chains in this region. Assuming that the molecular field caused by the disordered chains is strictly zero, the interchain staggered field for this structure will be $3J'$ for $\frac{2}{3}$ of the chains and zero for the other $\frac{1}{3}$. To account for the rapid decay of in-plane correlations with increasing temperature, the interchain

TABLE IV. Probabilities of molecular fields.

Molecular field	Weight		Raman label
h	$T < T_{N_2}$	$T_{N_2} < T < T_{N_1}$	
h_0	$\frac{2}{3}$	$\frac{5}{12}$	C
$h_0 + 2J'$	0	$\frac{3}{12}$	B_2
$h_0 + 4J'$	0	$\frac{3}{12}$	B_1
$h_0 + 6J'$	$\frac{1}{3}$	$\frac{1}{12}$	A

TABLE V. Raman frequencies (in THz).

Experiment Frequency	Assignment[a]	Present fit Frequency	Present fit Comment	LBW[b] fit Frequency	LBW[b] fit Comment
		$CsCoBr_3$			
2.64	$1C$	2.60			Cannot fit
2.96	$1B2$	2.92		2.97	
3.42	$2B2$	3.41	One value,	3.42	Used $\epsilon=0.185$
4.07	$4B2$	4.10	$\epsilon=0.137$,	4.07	
4.62	$6B2$	4.63	fits all	4.58	
3.10	$1B1$	3.13	lines	3.11	
3.81	$2B1$	3.81		3.84	Used $\epsilon=0.210$
4.35	$3B1$	4.33		4.40	
3.21	$1A$	3.30		3.23	Used $\epsilon=0.235$
4.18	$2A$	4.15		4.20	
4.84	$3A$	4.82		4.93	
LBW[b] use: $J=1.89$ THZ, $J'/J=0.019$					
Present fit: $J=1.62$ THz, $J'/J=0.059$, $h_0/J=0.020$					
		$CsCoCl_3$			
2.46	$1C$	2.45			Cannot fit
2.60	$1B2$	2.58		2.60	
2.83	$2B2$	2.83	One value,	2.83	
3.03	$3B2$	3.03	$\epsilon=0.120$,	3.00	Used $\epsilon=0.112$
3.15	$4B2$	3.20	fits all	3.14	
3.39	$5B2$	3.35	lines	3.39	Assigned $6B2$
3.49	$6B2$	3.49		3.50	Assigned $7B2$
2.66	$1B1$	2.67		2.67	
3.00	$2B1$	3.01		3.02	Used $\epsilon=0.128$
3.27	$3B1$	3.28		3.30	
3.49	$4B1$	3.50		3.53	
2.72	$1A$	2.75		2.72	
3.20	$2A$	3.16		3.20	Used $\epsilon=0.144$
3.49	$3A$	3.48		3.56	
LBW[b] use: $J=1.50$ THz, $J'/J=0.0125$					
Present fit: $J=1.495$ THz, $J'/J=0.020$, $h_0/J=0.013$					

[a]For explanation of the notation used to assign the lines of the Zeeman ladder (see Ref. 15).
[b]Reference 15.

molecular field is expected to vary as $h_{ic}=3J'e^{-\kappa_1}\equiv 3J'_{eff}$ for $\frac{2}{3}$ of the chains and zero for the remaining $\frac{1}{3}$.

The spin-wave response for $CsCoBr_3$ and $CsCoCl_3$ at 35 and 25 K, respectively, were then calculated as follows. The parameter J was fixed at the value obtained from the high-temperature fit, and ϵ was fixed by the fit to the low-temperature Raman data. The single-ion staggered field h_0 was assumed to decrease with temperature by a factor $e^{-\kappa}=\tanh(\beta J/2)$, where κ is the Ising inverse correlation length along the chain. Assuming that $\frac{2}{3}$ of the chains have staggered fields $h=h_0+3J'_{eff}$, and the other $\frac{1}{3}$ have $h=h_0$, J'_{eff} was varied to fit the observed scattering at the antiferromagnetic zone center.

Figures 15 and 16 show the results of the fits to the zone center of $CsCoBr_3$ and $CsCoCl_3$ in the intermediate-temperature region. The solid line is the theoretical expression convoluted with a Gaussian spectrometer resolution function and scaled to the data. The points are data from which a uniform fast-neutron background has been subtracted. The calculations were done for a ring of 80 spins; in

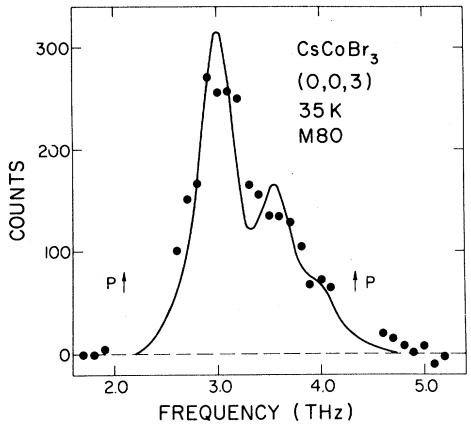

FIG. 15. $CsCoBr_3$ antiferromagnetic zone-center spin-wave response in the intermediate-temperature regime. Theoretical line is described in the text. Arrows mark positions of phonon scattering not included in the fit.

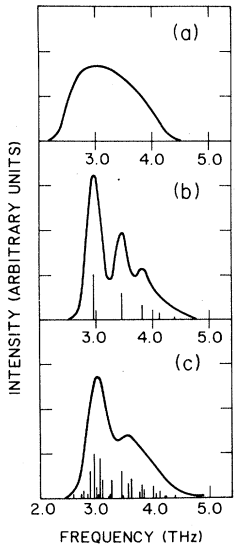

FIG. 17. Effect of fluctuating staggered field on the zone-center spin-wave response. (a) No field, $h=0$. (b) Single field, $h\neq 0$. (c) Field with fluctuations included by a Gaussian weighting of possible configurations. Histograms show $S^{xx}(Q,\omega)$, the solid lines are $S^{xx}(Q,\omega)$ convoluted with a Gaussian to simulate spectrometer resolution.

practice no variation of the line shape could be detected when 40 or more spins were included.

The theory gives a very good account of the zone-center response observed at (0,0,3) for $CsCoBr_3$. The sharp peak at the low-frequency end of the spectrum (Fig. 15) is well reproduced as is the overall extent of the scattering. The calculated structure is, however, somewhat too pronounced. The calculation is not as good for the (1,0,1) response of $CsCoCl_3$ (Fig. 16). The spectral weight of the low-frequency peak is underestimated relative to the high-frequency tail. The agreement, however, is much better than the $h=0$ IS theory (for a comparison see Fig. 17 or Ref. 11). The model satisfactorily accounts for the main features of the scattering. The crystal of $CsCoCl_3$ used had a somewhat

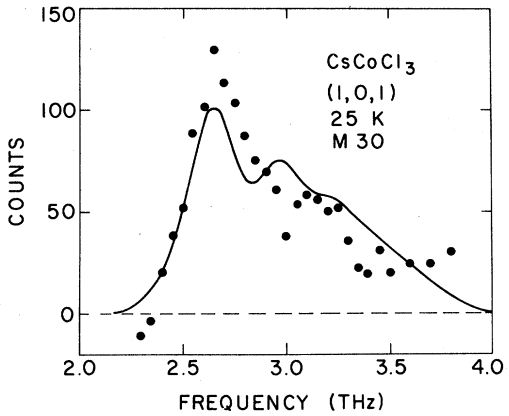

FIG. 16. $CsCoCl_3$ antiferromagnetic zone-center spin-wave response in the intermediate-temperature regime. Theoretical line is described in the text.

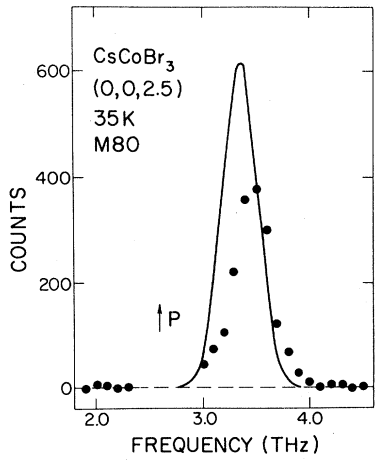

FIG. 18. $CsCoBr_3$ zone-boundary spin-wave response in the intermediate-temperature region. Theoretical line is described in the text.

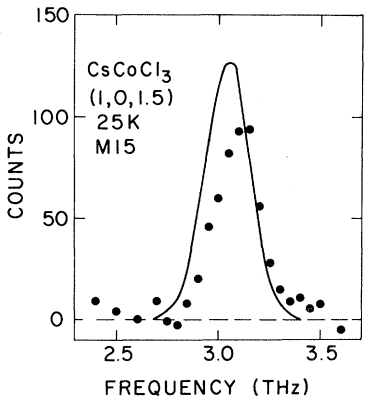

FIG. 19. $CsCoCl_3$ zone-boundary response in the intermediate-temperature region. Theoretical line is described in the text.

for $CsCoCl_3$ at 25 K. These values are quite reasonable considering the Ginzburg criterion discussed earlier. The calculation is scaled by an arbitrary constant S_T, and this should serve as a measure of the depopulation of the ground state. Again, using the simple estimate given by the single-ion ground-state populations, one expects for $CsCoBr_3$ at 35 K that

$$(S_{77}/S_{35})_{\mathrm{Br}}=\left[\frac{1+e^{-2J/35k_B}}{1+e^{-2J/77k_B}}\right]=0.89\ .$$

For $CsCoCl_3$ at 25 K one expects $(S_{50}/S_{25})_{\mathrm{Cl}}=0.86$. The observed values are, for $CsCoBr_3$, $(S_{77}/S_{35})_{\mathrm{obs}}=0.65$, and for $CsCoCl_3$, $(S_{50}/S_{25})_{\mathrm{obs}}=0.78$, indicating that thermal depopulation is somewhat underestimated by the procedure used above.

We have ignored fluctuations in the local molecular field. Fluctuations could be included in a qualitative way by assuming some distribution of fields in the paramagnetic region, such as a Gaussian,

$$\exp\left[-\left[\frac{(h-\langle h\rangle)^2}{2\langle h\rangle^2}\right]\right].$$

The result of this would be to broaden out and round off the observed scattering as shown qualitatively in Fig. 17. This may explain the width of the main peak, especially in the $CsCoBr_3$ scan.

Figures 18 and 19 show a comparison of the same theory with the observed zone-boundary scattering in $CsCoBr_3$ and $CsCoCl_3$. The solid lines are the same theory as in Figs. 15 and 16, corrected for monitor, form factor, and polarization factor. The data are corrected for fast-neutron background. Qualitatively, the theory predicts the narrow width observed at the zone boundary. However, the frequency of the zone-boundary mode is slightly underestimated and the relative intensity at the zone boundary is somewhat overestimated.

Part of the frequency difference may arise because all parameters were estimated by fitting only to the zone-center scattering. This was a deliberate restriction so as to bring out any internal inconsistency in the theory. In particular, the exchange constant J was obtained from the high-temperature scans at the zone center. If at 35 K, J is increased slightly the zone-boundary frequency can be matched exactly. If ϵ at 35 K is correspondingly increased the zone-center fit will still be satisfactory. On the other hand, it is more difficult to account for the intensity difference. The first-order perturbation-theory calculation of the spin-wave response underestimates the intensity variation as a function of Q.[8–10] The theory gives a ratio of structure factors at (0,0,2) and at (0,0,3) of 0.57, while our experiment shows the ratio to be 0.43 ± 0.06. Notwithstanding the improvement made by including exchange mixing and 3D correlations, our results therefore show that a more complete theory of the response of the bare 1D chain is necessary. The essential physics of the spin-wave response, however, can be understood in terms of the present model. The peak at the low-frequency end of the zone-center scattering is largely due to the effect of 3D correlations on the response of the quasi-1D antiferromagnetic chains. These correlations are important in the paramagnetic region when T is slightly greater than T_{N_1}. The field from single-ion exchange mixing is about half as large.

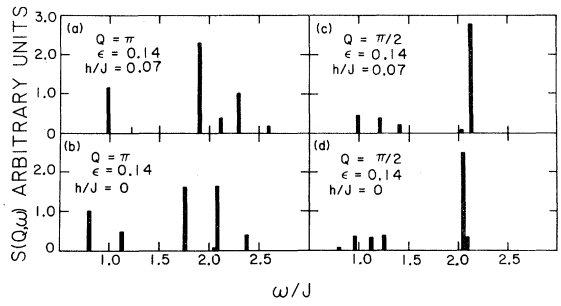

FIG. 20. $S^{xx}(Q,\omega)$ at $T=0$ for an open-ended chain of eight spins. Response near $\omega\sim J$ vanishes in the limit of large N. Asymmetry of the spin-wave response near $\omega\sim 2J$ is strongly enhanced by the addition of a small staggered-field term.

A. Exact calculations

As a complementary calculation to the one presented above we have performed an exact calculation of $S^{xx}(Q,\omega)$ for a chain of eight $S=\frac{1}{2}$ spins

with open ends. Figure 20 shows the $T=0$ calculation for the Ising-type antiferromagnet with and without a uniform staggered field. The spectral weight at $\omega \sim J$ will vanish in the limit $N \to \infty$. A small staggered field strongly enhances the low-frequency component of the response near $2J$. This exact calculation demonstrates that the qualitative change in $S^{xx}(Q,\omega)$ in the presence of the field is not a special feature of the first-order calculation. Any improved calculation of $S^{xx}(Q,\omega)$ for the bare exchange Hamiltonian will have the asymmetry enhanced by the inclusion of this term.

V. SUMMARY

The spin-wave response in the quasi-1D Ising-type antiferromagnets $CsCoCl_3$ and $CsCoCl_3$ has been measured by inelastic neutron scattering. The highly asymmetric line shapes cannot be described by previous theories to order ϵ. An improved effective $S=\frac{1}{2}$ spin Hamiltonian has been derived for these salts that includes staggered-field terms from exchange mixing and from 3D correlations. The interchain correlations are found to be important even in the paramagnetic-temperature region. When the interchain effects are accounted for in a mean-field approximation a first-order perturbation calculation of $S^{xx}(Q,\omega)$ can explain the essential features of the spin-wave response in the paramagnetic region from temperatures of $T \gtrsim T_{N_1}$ to $T \sim J/k_B$. In addition, the Raman scattering frequencies observed in the magnetically ordered region are well accounted for. Results of exact calculations for chains of eight spins with open ends confirm the effects of the internal fields on the spectral asymmetry.

ACKNOWLEDGMENTS

The expert technical assistance of J. C. Evans and H. F. Nieman is gratefully acknowledged. We thank J. C. Bonner, G. Müller, I. Johnstone, and D. J. Lockwood for useful discussions. One of the authors (S.E.N.) was supported by a Natural Sciences and Engineering Research Council of Canada (NSERC) scholarship. Thanks are due to A. Furrer and U. Tellenbach for the loan of the crystal of $CsCoCl_3$.

[1]J. C. Bonner, H. W. J. Blöte, H. Beck, and G. Müller, in *Physics in One Dimension,* edited by J. Bernasconi and T. Schneider (Springer, New York, 1981).
[2]M. Steiner, in *Physics in One Dimension,* Ref. 1.
[3]M. Steiner, J. Villain, and C. G. Windsor, Adv. Phys. 25, 87 (1976).
[4]M. Melamud, H. Pinto, J. Makovsky, and H. Shaked, Phys. Status Solidi B 63, 699 (1974).
[5]M. Mekata and K. Adachi, J. Phys. Soc. Jpn. 44, 806 (1978).
[6]W. B. Yelon, D. E. Cox, and M. Eibschütz, Phys. Rev. B 12, 5007 (1975).
[7]N. Achiwa, J. Phys. Soc. Jpn. 27, 561 (1969).
[8]U. Tellenbach, J. Phys. C 11, 2287 (1978).
[9]K. Hirakawa and H. Yoshizawa, J. Phys. Soc. Jpn. 46, 455 (1979).
[10]W. J. L. Buyers, J. Yamanaka, S. E. Nagler, and R. L. Armstrong, Solid State Commun. 33, 857 (1980).
[11]S. E. Nagler, R. L. Armstrong, and W. J. L. Buyers, J. Appl. Phys. 52, 1971 (1981).
[12]S. K. Satija, G. Shirane, H. Yoshizawa, and K. Hirakawa, Phys. Rev. Lett. 44, 1548 (1980).
[13]H. Yoshizawa, K. Hirakawa, S. K. Satija, and G. Shirane, Phys. Rev. B 23, 2298 (1981).
[14]A. Brun, P. Mayer, and B. Briat, J. Phys. C 13, 5575 (1980).
[15]W. P. Lehmann, W. Breitling, and R. Weber, J. Phys. C 14, 4655 (1981).
[16]I. W. Johnstone, D. J. Lockwood, and M. W. C. Dharma-Wardana, Solid State Commun. 36, 5934 (1980).
[17]J. Villain, Physica 79B, 1 (1975).
[18]N. Ishimura and H. Shiba, Prog. Theor. Phys. 63, 745 (1980).
[19]M. Fowler, J. Phys. C 11, 2977 (1978).
[20]J. des Cloizeaux and M. Gaudin, J. Math. Phys. 7, 1384 (1966).
[21]S. E. Nagler, W. J. L. Buyers, R. L. Armstrong, and B. Briat, Phys. Rev. Lett. 49, 590 (1982).
[22]J. J. Johnson, S. Krinsky, and B. M. McCoy, Phys. Rev. A 8, 2516 (1973).
[23]I. W. Johnstone, G. D. Jones, and D. J. Lockwood, Solid State Commun. 39, 395 (1981).
[24]M. E. Lines, Phys. Rev. 131, 546 (1963).
[25]H. M. Gladney, Phys. Rev. 146, 253 (1966).
[26]W. J. L. Buyers, T. M. Holden, E. C. Svensson, R. A. Cowley, and M. T. Hutchings, J. Phys. C 4, 2139 (1971).
[27]W. J. L. Buyers, T. M. Holden, and D. J. Lockwood (private communication) have found that the bare interaction between isolated pairs of Co^{2+} ions is isotropic to a few percent.
[28]H. Shiba, Prog. Theor. Phys. 64, 466 (1980).
[29]H. Yoshizawa and K. Hirakawa, J. Phys. Soc. Jpn. 46, 448 (1979).
[30]J. H. M. Thornley, C. G. Windsor, and J. Owen, Proc. R. Soc. London Ser. A 284, 252 (1965).
[31]D. Scalapino, Y. Imry, and P. Pincus, Phys. Rev. B 11, 2042 (1975).